



# Omega-3 fatty acids decrease CRYAB, production of oncogenic prostaglandin E<sub>2</sub> and suppress tumor growth in medulloblastoma

Linda Ljungblad<sup>a,\*</sup>, Filip Bergqvist<sup>b</sup>, Conny Tümmeler<sup>a</sup>, Samantha Madawala<sup>c</sup>, Thale Kristin Olsen<sup>a</sup>, Teodora Andonova<sup>a</sup>, Per-Johan Jakobsson<sup>b</sup>, John Inge Johnsen<sup>a</sup>, Jana Pickova<sup>c</sup>, Birgitta Strandvik<sup>d</sup>, Per Kogner<sup>a,e</sup>, Helena Gleissman<sup>a</sup>, Malin Wickström<sup>a</sup>

<sup>a</sup> Childhood Cancer Research Unit, Department of Women's and Children's Health, Karolinska Institutet, Stockholm, Sweden

<sup>b</sup> Division of Rheumatology, Department of Medicine, Solna, Karolinska Institutet, and Karolinska University Hospital, Stockholm, Sweden

<sup>c</sup> Department of Molecular Sciences, Swedish University of Agricultural Sciences, Uppsala, Sweden

<sup>d</sup> Department of Biosciences and Nutrition Karolinska Institutet, NEO, Flemingsberg, Stockholm, Sweden

<sup>e</sup> Pediatric Oncology, Astrid Lindgrens Childrens Hospital, Karolinska University Hospital, Stockholm, Sweden

## ARTICLE INFO

### Keywords:

Docosahexaenoic acid  
Eicosapentaenoic acid  
Docosapentaenoic acid  
Dihomo- $\gamma$ -linolenic acid  
Prostacyclin  
Thromboxane  
Pediatric cancer  
CRYAB

## ABSTRACT

**Aims:** Medulloblastoma (MB) is one of the most common malignant central nervous system tumors of childhood. Despite intensive treatments that often leads to severe neurological sequelae, the risk for resistant relapses remains significant. In this study we have evaluated the effects of the  $\omega$ 3-long chain polyunsaturated fatty acids ( $\omega$ 3-LCPUFA) docosahexaenoic acid (DHA) and eicosapentaenoic acid (EPA) on MB cell lines and in a MB xenograft model.

**Main methods:** Effects of  $\omega$ 3-LCPUFA treatment of MB cells were assessed using the following: WST-1 assay, cell death probes, clonogenic assay, ELISA and western blot. MB cells were implanted into nude mice and the mice were randomized to DHA, or a combination of DHA and EPA treatment, or to control group. Treatment effects in tumor tissues were evaluated with: LC-MS/MS, RNA-sequencing and immunohistochemistry, and tumors, erythrocytes and brain tissues were analyzed with gas chromatography.

**Key findings:**  $\omega$ 3-LCPUFA decreased prostaglandin E<sub>2</sub> (PGE<sub>2</sub>) secretion from MB cells, and impaired MB cell viability and colony forming ability and increased apoptosis in a dose-dependent manner. DHA reduced tumor growth *in vivo*, and both PGE<sub>2</sub> and prostacyclin were significantly decreased in tumor tissue from treated mice compared to control animals. All  $\omega$ 3-LCPUFA and dihomogamma-linolenic acid increased in tumors from treated mice. RNA-sequencing revealed 10 downregulated genes in common among  $\omega$ 3-LCPUFA treated tumors. CRYAB was the most significantly altered gene and the downregulation was confirmed by immunohistochemistry.

**Significance:** Our findings suggest that addition of DHA and EPA to the standard MB treatment regimen might be a novel approach to target inflammation in the tumor microenvironment.

## 1. Introduction

Medulloblastoma (MB) is one of the most common malignant tumors in the central nervous system (CNS) in childhood and arises in or near the cerebellum. Most children with MB undergo intensive multimodal

therapy, including surgery, craniospinal radiotherapy and chemotherapy, which has considerably improved survival [1,2]. Unfortunately, this intense treatment regimen during childhood often results in significant long-term neurological morbidity that increases with age [3]. In addition, the risk of relapse is significant [4]. In recent years,

**Abbreviations:** AA, arachidonic acid; CNS, central nervous system; COX, cyclooxygenase; DGLA, dihomogamma-linolenic acid; DHA, docosahexaenoic acid; DPA,  $\omega$ 3-docosapentaenoic acid; EPA, eicosapentaenoic acid; ELISA, enzyme-linked immunosorbent assay; FBS, fetal bovine serum; FO, fish oil; GC, gas chromatography; 6kPGF<sub>1 $\alpha$</sub> , 6-keto-prostacyclin F<sub>1 $\alpha$</sub> ; LC-MS/MS, liquid chromatography with tandem mass spectrometry; MB, medulloblastoma; MB<sub>SHH</sub>, sonic Hedgehog group; MB<sub>WNT</sub>, the wingless group; mPGES-1, microsomal prostaglandin E synthase-1;  $\omega$ 3-LCPUFA, omega-3 long chain polyunsaturated fatty acids; PGI<sub>2</sub>, prostacyclin; PGE<sub>2</sub>, prostaglandinE<sub>2</sub>; RBC, red blood cells; SHH, sonic hedgehog; SEM, standard error of the mean; SD, standard deviation; TxA<sub>2</sub>, thromboxane A<sub>2</sub>; TxB<sub>2</sub>, thromboxane B<sub>2</sub>; TME, tumor microenvironment; WST-1, water soluble tetrazolium salts.

\* Corresponding author at: Department of Women's and Children's Health, Karolinska Institutet, Tomtebodavägen 18A, S-17177 Stockholm, Sweden.

E-mail address: [linda.ljungblad@ki.se](mailto:linda.ljungblad@ki.se) (L. Ljungblad).

<https://doi.org/10.1016/j.lfs.2022.120394>

Received 29 September 2021; Received in revised form 5 February 2022; Accepted 7 February 2022

Available online 11 February 2022

0024-3205/© 2022 The Authors. Published by Elsevier Inc. This is an open access article under the CC BY license (<http://creativecommons.org/licenses/by/4.0/>).

molecular characterization has led to the identification of four major, clinically relevant, MB subclasses based on their gene expression profiles: the wingless group (MB<sub>Wnt</sub>), the Sonic Hedgehog group (MB<sub>SHH</sub>), group 3 and group 4 [5,6]. The groups differ in regard to oncogenic drivers, clinical characteristics and outcome, and should be considered as different disease entities, although, some have described group 3 and group 4 as a mixed subgroup of patients. Furthermore, single cell RNA-sequencing recognized undifferentiated and differentiated neuronal-like malignant populations across the MB subgroups [7,8]. Despite extensive characterization, effective subgroup-specific therapies have yet to emerge emphasizing the need for a deeper understanding of MB. Single cell RNA-sequencing indicates that MB<sub>SHH</sub> has the most distinct immune signature with significantly higher proportions of myeloid cell populations [9]. Furthermore, syngeneic MB<sub>SHH</sub> animal models demonstrated a more pronounced infiltration of myeloid cells and lymphocytes into the tumor compared to MB<sub>group3</sub> [10].

Inflammation plays an important role in initiating anti-tumorigenic immune responses, however, dysregulated inflammation in the tumor microenvironment (TME) can suppress the anti-tumor immune responses, promote angiogenesis and facilitate invasion and metastasis [11,12]. Prostaglandin E2 (PGE<sub>2</sub>) is a potent pro-inflammatory and immunosuppressive lipid mediator synthesized from the  $\omega$ -6-fatty acid arachidonic acid (AA) by the key enzymes cyclooxygenase (COX) -1 and -2, and the terminal enzyme microsomal prostaglandin E synthase-1 (mPGES-1) [13]. It is well-established that the COX/mPGES-1/PGE<sub>2</sub> pathway is upregulated in several cancers including colorectal cancer, non-small cell lung cancer, breast cancer, MB and neuroblastoma [14–18]. PGE<sub>2</sub> drives immune evasion by modulating the microenvironment into a more tolerant state and suppressing immune responses in both the innate and adaptive immune compartments [19–21]. Furthermore, PGE<sub>2</sub> contributes to the formation of micrometastases during early tumor development [22]. Consequently, inhibition of PGE<sub>2</sub> production has emerged as a promising therapeutic approach in brain tumors such as glioblastoma and MB [18,23]. Pharmacological inhibition of PGE<sub>2</sub> production or signaling reduced MB growth both *in vitro* and *in vivo* and tumors from MB patients displayed high expression of COX-2, mPGES1 and all four PGE<sub>2</sub> receptors [18]. Additionally, PGE<sub>2</sub> has been detected in plasma of pediatric patients with brain tumors at the time of surgery, and in supernatants from primary MB cultures [24]. Inhibition of COX-2, by celecoxib in MB-derived cell cultures enhanced the response to high-dose radiation *in vitro* and *in vivo* in immunocompromised mice [25]. Furthermore, dying cancer cells elevate PGE<sub>2</sub> levels in the TME following chemotherapy [26] and increased levels of PGE<sub>2</sub>, caused by chemotherapy, have shown to generate chemoresistance by stimulating cancer stem cells to repopulate the tumor [27]. Overall, limiting PGE<sub>2</sub> production is an attractive treatment approach for cancer in general and MB in particular.

A potential therapeutic approach to decrease PGE<sub>2</sub> in cancer tissues is an increased intake of omega-3 long chain polyunsaturated fatty acids ( $\omega$ 3-LCPUFA), for example docosahexaenoic acid (DHA). This has previously been demonstrated in neuroblastoma [28]. Additionally, DHA and the  $\omega$ 3-LCPUFA eicosapentaenoic acid (EPA) have demonstrated anti-proliferative properties in cancer cells, both when given separately and together, by affecting survival and death signals, specifically by inducing apoptotic signaling and increasing oxidative stress [29–31]. Moreover, a recent meta-analysis has shown that high concentrations of  $\omega$ 3-LCPUFA are associated with lower cancer-related mortality [32] and clinical trials have demonstrated that  $\omega$ 3-supplementation ameliorates cancer-related symptoms including neuropathy and inflammation with overall improvement in the quality of life [33]. The  $\omega$ 3-LCPUFA are of particular interest in the context of brain cancers as they can easily cross the blood-brain barrier and have been reported to reduce tumor growth, angiogenesis and metastases in glioma and brain metastases models of melanoma, whereas treatment with PGE<sub>2</sub> displayed the opposite effect [34]. Notably, DHA has also been shown to sensitize MB cells to chemotherapeutic agents [35]. These studies indicate that  $\omega$ 3-

LCPUFA may be a possible novel treatment option for MB patients that could serve as a complement to the current protocols. Thus, we set out to investigate the potential of DHA and EPA for the treatment of MB and their effect on prostaglandin production *in vitro* and *in vivo*. Here, we report that treatment with  $\omega$ 3-LCPUFA suppressed MB growth and induced cell death. In addition, we also observed an altered fatty acid composition and reduced levels of PGE<sub>2</sub>, accompanied by a decreased expression of CRYAB in the tumors after  $\omega$ 3-LCPUFA treatment.

## 2. Material and methods

### 2.1. Cell lines

Six human MB cell lines derived from different MB subgroups were used in this study; SHH: DAOY and UW228-3, Group 3: Med8a, D425, D458 and Group 3/4: D283 (Table S1). DAOY and D283 were purchased from ATCC (ATCC-LGC Standards, Middlesex, UK) and D425, D458 and Med8a were kindly provided by Dr. M. Nistér (Karolinska Institutet). The cells were cultured as follow: Minimal essential Media (MEM) for DAOY and D283, Dulbecco's modified Eagle's medium (DMEM) for Med8a, improved MEM with zinc/DMEM for D425 and D458 and DMEM/F12 for UW228-3 [36]. Media was supplemented with 2 mM L-glutamine, 100 IU/mL penicillin G, 100  $\mu$ g/mL streptomycin and 10% (or 15% Med-8a, D425, D458) heat-inactivated fetal bovine serum (FBS). The cells were grown at 37 °C in a humidified 5% CO<sub>2</sub> atmosphere. Media and supplements were purchased from Gibco (Life Technologies, Thermo Fisher Scientific Inc). Cells were authenticated using short tandem repeat analysis AmpFISTR® Identifier™ PCR Amplification Kit (Applied Biosystems, Thermo Fisher Scientific) and routinely tested for mycoplasma (EZ-PCR Mycoplasma Test Kit, Biological industries).

### 2.2. EPA and DHA *in vitro*

For the assessment of EPA and DHA efficacy *in vitro*, different concentrations of EPA and DHA (0.625, 1.25, 2.50, 5.00, 10.0, 20.0, 40.0, 80.0, 160  $\mu$ M) were added to RPMI medium containing 10% FBS. DHA and EPA were purchased from Nu-ChekPrep (Elysian) and arachidonic acid (AA) was bought from Sigma-Aldrich. The fatty acids were dissolved in 99.5% ethanol.

### 2.3. Cell viability assay

Cell viability of cells grown in monolayer or suspension was assessed using the colorimetric, formazan-based WST-1 assay (Roche, Sigma-Aldrich). Cells were seeded in 96-well plates (5000–15,000 cells/well) and adherent cells were left to attach for 24 h prior to treatment with DHA or EPA (0.625–80.0  $\mu$ M) for 72 h. The assay was repeated at least three times with all concentrations being tested in triplicates. Analyses were performed according to manufacturer instructions and absorbance was measured at 450 nm and with a reference measurement at 650 nm using a VersaMax reader (Molecular Devices). Results are presented, with blank subtracted, as percent relative to untreated control  $\pm$  standard error of the mean (SEM).

### 2.4. Tumor spheroid culture, cell death and viability assays

For 3D tumor spheroids cells DAOY and UW228-3 were dissociated into single cell suspension and seeded into ultra-low attachment round bottom 96-well plate (Corning # 4515) at a density of 500 and 1500 cells/well, respectively, in 100  $\mu$ L neurosphere medium (Advanced DMEM/F-12), 2% B-27 supplement, 1% N-2 supplement, 2  $\mu$ g/mL Heparin, 20 ng/mL Epidermal Growth Factor, and 10 ng/mL basic Fibroblast Growth Factor (Thermo Fisher Scientific) as described in [37]. After 24 h when tumor spheroids had formed, two-fold concentration of DHA, EPA or vehicle (ethanol) in a 100  $\mu$ L neurosphere

media were added to each well (final concentration of 10–160  $\mu\text{M}$ ). After 72 h a second cycle of treatment was added, replenishing 100  $\mu\text{L}$  of the media with vehicle or DHA and EPA. Cell viability was analyzed using CellTiter-Glo® 3D Cell Viability Assay (Promega) according to the manufacturer's protocol 6 days after the first treatment. Luminescence was measured using the Varioskan™ LUX plate reader (Thermo Fisher Scientific). Cell death in 3D tumor spheroids was assessed by SYTOX™ Green Nucleic Acid Stain (Thermo Fisher Scientific) that was added to the tumor spheroids during treatment at a final concentration of 12.5 nM. The nucleic acid stain enters cells with compromised membranes and emits fluorescence when binding to DNA, as a measurement of dying cells. Green fluorescence intensity was assessed and tumor spheroid growth was monitored using the Incucyte® S3 Live-Cell Analysis Instrument (Sartorius). The experiment was repeated three times with five replicates at each concentration.

## 2.5. Colony formation assay

Single-cell suspensions of DAOY or UW228-3 cells were seeded in 6-well plates (Cell+, Sarstedt) at a density of 150–175 cells/well. Cells were allowed to attach for 24 h and treated in triplicates with three concentrations of DHA (DAOY: 10, 20 and 40  $\mu\text{M}$  and UW228-3: 40, 80 and 160  $\mu\text{M}$ ) for 72 h. Afterwards, media was replaced with drug-free medium and the cells were grown for approximately 7 days [38]. When the colonies reached a size of >50 cells the plates were washed with PBS (Thermo Fisher Scientific), fixed in 3.7–4.0% formaldehyde (PanReac AppliChem) and stained with Giemsa (Sigma-Aldrich). Clones containing >50 cells were counted, and the experiment was repeated two times. Data from three independent experiments is presented as % of control (mean  $\pm$  SEM).

## 2.6. Assessment of protein expression using Western blot

DAOY cells were seeded in 6-well plates (TPP Techno Plastic Products AG) in 1 mL cell culture media at a density of 75,000 cells/well and 30,000 cells/well for 24 h and 48 h treatments, respectively. Cells were allowed to attach overnight and treated with DHA, EPA or vehicle (final concentration DHA and EPA 10, 20, 40, 80, 160  $\mu\text{M}$ ). After 24 or 48 h incubation cells were washed briefly with PBS and harvested in RIPA buffer containing Halt™ Protease and Phosphatase Inhibitor Cocktail (Thermo Fisher Scientific). Samples were sonicated for 3 cycles (30s on/off) and cellular debris was removed by centrifugation at 14,000  $\times g$  for 10 min at 4 °C. Protein concentrations were determined using the DC Protein Assay (Bio-Rad) according to the user manual. The protein lysates were supplemented with Pierce™ Lane Marker Reducing Sample Buffer (Thermo Fisher Scientific) and incubated for 10 min at 70 °C. Equal amounts of protein were separated on NuPAGE™ 4 to 12%, Bis-Tris gels (Thermo Fisher Scientific) and transferred onto a Immobilon-P Membrane, PVDF, 0.45  $\mu\text{m}$  (Merck Millipore). The membranes were blocked in TBS-T (Tris-buffered saline (TBS) with 0.1% Tween-20; Sigma-Aldrich) containing 5% (w/v) Nonfat Dry Milk (Cell Signaling Technology, CST). The membranes were incubated with the primary antibodies (anti-PARP, #9542, CST; anti-vinculin, #ab129002, Abcam) in blocking buffer overnight at 4 °C (anti-PARP) or for 1 h at room temperature (anti-vinculin). Following washes in TBS-T, the membranes were incubated with the secondary antibody (anti-rabbit IgG, HRP-linked) for 1 h. Detection and visualization were performed using SuperSignal™ West Pico PLUS Chemiluminescent Substrate (Thermo Fisher Scientific) and iBright FL1000 Imaging System (Thermo Fisher Scientific). Precision Plus Protein Dual Color Standard (Bio-Rad) and MagicMark™ XP (Thermo Fisher Scientific) were used to estimate the molecular mass of the detected proteins. Stripping was performed according to the manufacturer's instructions using Restore™ PLUS Western Blot Stripping Buffer (Thermo Fisher).

## 2.7. Measurement of PGE<sub>2</sub> production in MB cell supernatants

Two human medulloblastoma cell lines DAOY and D283 were seeded in 96-well plates and cultivated in RPMI medium containing 10% FBS. After 24 h the cells were incubated with 80  $\mu\text{M}$  arachidonic acid (Sigma-Aldrich) for 24 h at 37 °C. After centrifugation, 5 min 1500 RPM at room temperature, the medium was exchanged to RPMI with 10% FBS containing increasing concentrations of DHA (5, 10 or 20  $\mu\text{M}$ ) and the cells were incubated for 24 h at 37 °C. Cell supernatants were collected and PGE<sub>2</sub> levels in the cell supernatant were assessed using a PGE<sub>2</sub> Enzyme-linked immunosorbent assay (ELISA) kit (Cayman Chemicals) according to the manufacturer's instructions. Optical density was assessed at a wavelength of 415 nm using a VersaMax plate reader (Molecular Devices).

## 2.8. Medulloblastoma xenograft studies

The animal experiment was approved by the regional ethics committee for animal research (approval ID: N391/11) appointed under the control of the Swedish Board of Agriculture and the Swedish Court and conducted in accordance with the national regulations (SFS 1988:534, SFS 1988:539 and SFS 2009:1464) and the ARRIVE guidelines. Immunodeficient female nude mice (5–6-week-old NMRI nu/nu purchased from Scanbur) were left to acclimatize one week prior to subcutaneous injection on the flank with  $7.5 \times 10^6$  DAOY cells under general anesthesia (average body weight 22 g, range 21–24 g). Tumor volumes ( $V = \text{width}^2 \times \text{length} \times 0.44$ ) [39] were measured using a caliper and recorded every other day. When the tumor reached a volume of 150 mm<sup>3</sup> (mean 160 mm<sup>3</sup>, range 150–190 mm<sup>3</sup>), the mice were randomized into two treatment groups and one control group (group<sub>CTRL</sub>,  $n = 9$ ). The treatment groups received either DHASCO oil (DSM) (group<sub>DHA</sub>,  $n = 8$ ) containing 44.5% DHA (Table S2) given daily orally through gastric feeding or fish oil (FO) enriched fruit juice (Smartfish AS) (group<sub>FO</sub>,  $n = 8$ ) (Table S3). FO enriched fruit juice was changed daily and the bottles were weighed to estimate how much the mice drank. Mice in all groups ate normal chow (R36, R70 from Lantmännen). The dosing was chosen based on previous experience in our group [40] and mice in both treatment groups received a dose of approximately 1500 mg/kg (corresponding to a human equivalent dose of about 122 mg/kg [41]) daily for 30 days. The mice were continuously monitored for weight loss and signs of toxicity continuous. After 30 days, the mice were euthanized using carbon dioxide (CO<sub>2</sub>) in accordance to the EU regulation 2010/63/EU and after sacrifice blood was drawn from the heart. Brains and tumors were resected and weighed, the tissues were divided into pieces to be snap frozen and stored at –80 °C or fixed in 4% formaldehyde for histological analysis.

### 2.8.1. Fatty acid analyses with gas chromatography (GC)

Fatty acid concentrations in red blood cells (RBC), plasma, tumors, and brain tissue from the *in vivo* study were analyzed with gas chromatography (GC). Blood drawn at time of sacrifice was centrifuged at 4500 rpm (1000g) for 5 min and separated into cells and plasma and lipid extraction was performed from fresh material as previously described [42]. Tissue samples from brain and tumor were snap frozen after dissection and stored in –80 °C until analysis. Lipids from the tissues (100–250 mg tissue pieces) were extracted according to Hara and Radin [43]. In brief, tissue samples were homogenized manually in a glass homogenizer and lipids were extracted using 3  $\times$  1 mL of hexane–isopropanol (3:2), rinsing twice with 2  $\times$  3 mL of the solvent. After homogenization, 5 mL solvent was used for rinsing the vessel, 5 mL aqueous Na<sub>2</sub>SO<sub>4</sub> (6.67%) was added, and the tubes were manually shaken. After centrifugation, the upper layer was removed and dried under nitrogen and the lipids were dissolved in hexane and stored at –20 °C until further analysis. Total lipids were weighed on a microbalance (UMT2, Mettler Toledo), and total lipid content was determined. Internal fatty acid methyl ester standard was used (17:1,

Larodan) [44].

### 2.8.2. Prostanoid profiling in tumor tissue

Working on ice, snap frozen tumor tissue (25–50 mg) were spiked with 75  $\mu$ L of deuterated internal standards of 6-keto-PGF<sub>1 $\alpha$</sub> -d<sub>4</sub>, PGF<sub>2 $\alpha$</sub> -d<sub>4</sub>, PGE<sub>2</sub>-d<sub>4</sub>, PGD<sub>2</sub>-d<sub>4</sub>, TxB<sub>2</sub>-d<sub>4</sub>, and 15-deoxy- $\Delta^{12,14}$ PGJ<sub>2</sub>-d<sub>4</sub> (Cayman Chemical) in ethanol, 20  $\mu$ L of methanol, and made acidic with 125  $\mu$ L of 0.1% formic acid in milli-Q water. The tumors were homogenized by mechanical force with a pellet pestle (Kontes) and liquid extraction was performed by addition of 600  $\mu$ L of methanol, vortexing for 5 min, followed by centrifugation at 4000  $\times$ g for 5 min (4 °C) and collection of supernatants. The liquid extraction was repeated once. The extracted supernatants were evaporated under vacuum until <50  $\mu$ L remained and diluted in 1 mL 0.05% formic acid, 10% methanol in milli-Q water. Solid-phase extraction (SPE) was performed by loading samples on Oasis HLB 1cm<sup>3</sup> 30 mg cartridges (Waters) that had been preconditioned with 100% methanol and 0.05% formic acid in milli-Q water. The SPE columns were washed once with 10% methanol in milli-Q water followed by elution in 1 mL of 100% methanol. The samples were evaporated to dryness under vacuum and stored at –20 °C until reconstituted in 50  $\mu$ L of 7% acetonitrile, vortexed, centrifuged at 2500g for 2 min, and transferred to glass vials for analysis with liquid chromatography tandem mass spectrometry (LC-MS/MS). The injection volume was 20  $\mu$ L and analytes of interest were quantified using a triple quadrupole mass spectrometer (Acquity TQ detector, Waters) equipped with a 2795 Alliance HPLC (Waters). Separation was performed on a Synergi™ 2.5  $\mu$ m Hydro-RP 100 Å, 100  $\times$  2 mm column (Phenomenex) with a 45 min stepwise linear gradient (10–90%) at flow rate 0.2 mL/min with 0.05% formic acid in acetonitrile as mobile phase B and 0.05% formic acid in milli-Q water as mobile phase A. The column temperature was 55 °C. Individual prostanoids were measured in negative mode with multiple reaction monitoring method [45] Data were analyzed using MassLynx software, version 4.1, with internal standard calibration and quantification to external standard curves.

### 2.8.3. RNA-sequencing of tumor tissue

Bulk RNA-sequencing for the assessment of transcriptional changes in the tumor tissue was performed on a selection of tumors. The tumors were snap frozen and stored at 80 °C until analysis. The tissue was homogenized in 350–600  $\mu$ L RLT buffer (Qiagen) using a TissueLyser (Qiagen) with settings 2  $\times$  2 min/25.0. RNA was extracted from the lysate using the Qiagen RNeasy mini kit (Qiagen) according to the manufacturer's instruction. Library preparation was performed as follows: total RNA was subjected to quality and quantity control using Agilent Tapestation and Nanodrop. To construct libraries suitable for Illumina sequencing the Illumina TruSeq Stranded mRNA sample preparation protocol was used, which includes mRNA isolation, cDNA synthesis, ligation of adapters and amplification of indexed libraries. The yield and quality of the amplified libraries was analyzed using Qubit by Thermo Fisher and the Agilent Tapestation. The indexed cDNA libraries were normalized and combined, and the pools were sequenced on the Illumina Nextseq 550 for a 75-cycle v2 sequencing run generating 75 bp single-end reads. Basecalling and demultiplexing was performed using BCL2fastq v2.20 software with default settings generating Fastq files for further downstream mapping and analysis.

Further analysis was performed on tumors presenting high quality RNA and RNA Integrity Number (RIN)  $\geq$ 8, resulting in group<sub>CTRL</sub>  $n$  = 3, group<sub>FO</sub>  $n$  = 4, and group<sub>DHA</sub>  $n$  = 3. On average, a total of 11.8 million reads (range: 8.5–14.2 million) were obtained per sample. All samples had a mean Phred quality score of >30 across the entire read length. Raw sequencing .fastq files were aligned to the GRCh38 human reference genome applying the STAR 2-pass approach [46]. Aligned reads were quantified using htseq-count [47]. On average, 53% of unique, non-ambiguous assigned reads per sample (range: 46–60%) were used in gene expression quantification analyses. Differential gene expression was determined using DESeq2 [48]. After DESeq2 analysis, genes were

ranked by the sign of the log fold change and adjusted  $p$  value, an adjusted  $P$  value < 0.05 was considered significant.

### 2.8.4. Immunohistochemistry (IHC)

Following resection, tumor tissue was fixed in formaldehyde (3.7–4.0% w/v, (PanReac AppliChem)) for 24 h. Fixed tissues were processed in an automated tissue processor (LOGOS, Milestone), embedded in paraffin and 4  $\mu$ m FFPE sections (formalin-fixed, paraffin-embedded) were mounted on glass slides (Superfrost+, Thermo Scientific) and heated for 3 h at 56 °C. Following de-paraffinization in xylene and rehydration in series of graded alcohols, heat induced epitope retrieval (HIER) was performed in citrate buffer (pH 6, Sigma C-9999) using a Decloaking Chamber (Biocare Medical) set to 5 min at 110 °C. For quenching of endogenous peroxidase activity, tissues were incubated in 0.15% hydrogen peroxidase for 30 min at room temperature followed by a 30 min blocking step using 1% bovine serum albumin (BSA). Tissues were incubated with anti-Alpha B Crystallin (CRYAB) antibody (#ab226839, Abcam, diluted 1:400 in 1% BSA) in a humid chamber overnight at 4 °C. The secondary antibody, biotinylated anti-rabbit IgG (BA-1000, Vector Laboratories) was diluted 1:200 in TBS containing 0.02% Tween 20 and incubated for 30 min at room temperature. This was followed by a 30 min incubation with avidin-biotin enzyme complex (Vectastain ELITE ABC kit (HRP), Vector Laboratories). For visualization, slides were incubated with DAB substrate (ImmPACT DAB, SK-4105, Vector Laboratories) for 3 min. The sections were counterstained in Mayer's hematoxylin for 1 min followed by dehydration with graded alcohols and xylene and the slides were mounted with Mountex.

Sections were scanned at 40 $\times$  using the Axio Scan.Z1 Digital Slide Scanner (ZEISS). Image analysis was performed using QuPath v0.2.3 [49]. The positive cell detection function of QuPath was used to identify CRYAB-positive cells. Four hotspot areas were with comparable cell numbers were identified per tumor and the mean % of positive cells was calculated (mean 1290 cells/hotspot, standard deviation (SD) 130).

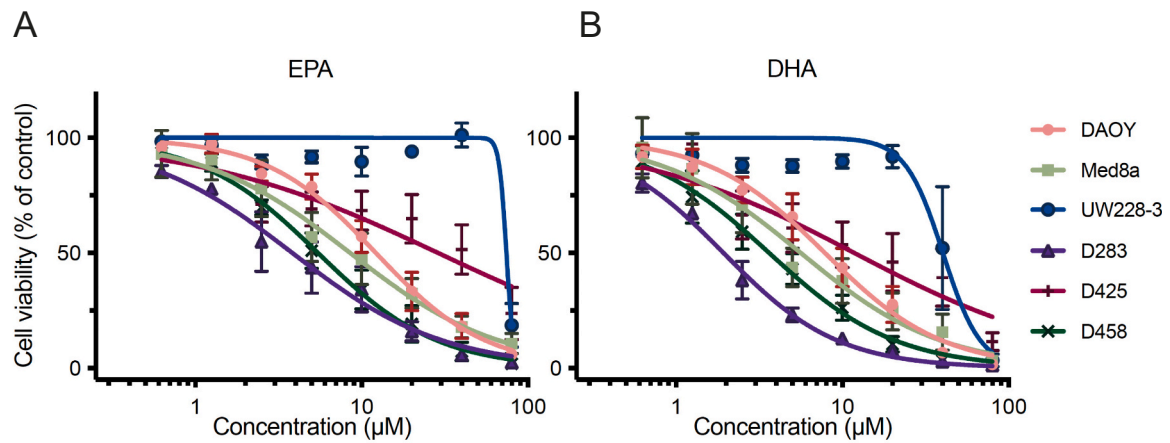
### 2.9. Statistical analyses

GraphPad Prism version 9.3.1 for Mac, GraphPad Software, San Diego, California USA, [www.graphpad.com](http://www.graphpad.com) was used for statistical analyses and graphs. IC<sub>50</sub> (inhibitory concentration 50%) values were calculated using non-linear regression on concentration-effect curves (model:  $Y = 100 / (1 + (IC_{50}/X)^{HillSlope})$ ). Unpaired  $t$ -test was used to test for statistical significance of IC<sub>50</sub> for DHA and EPA in individual cell lines, gene expression and IHC studies. For comparison for DHA and EPA in all cell lines simultaneously paired  $t$ -test was used on log IC<sub>50</sub>. The statistics analyzing clonogenic capacity were performed on raw data values. For comparison between two or more treatment groups/concentration levels to the control one-way ANOVA with Dunnett's multiple comparisons (MC) post-test was used. To identify outliers ROUT test was performed ( $Q = 1\%$ ).  $P < 0.05$  was considered statistically significant (\* $P < 0.05$ , \*\* $P < 0.01$ , \*\*\* $P < 0.001$  and, \*\*\*\* $P < 0.0001$ ).

## 3. Results

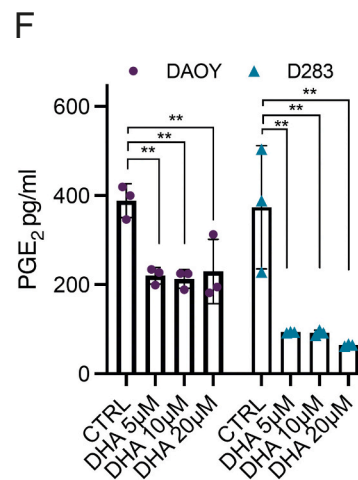
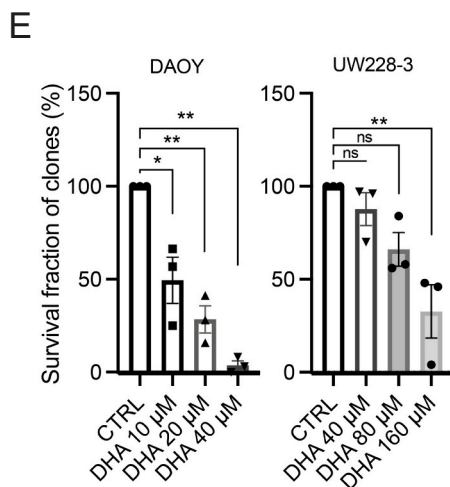
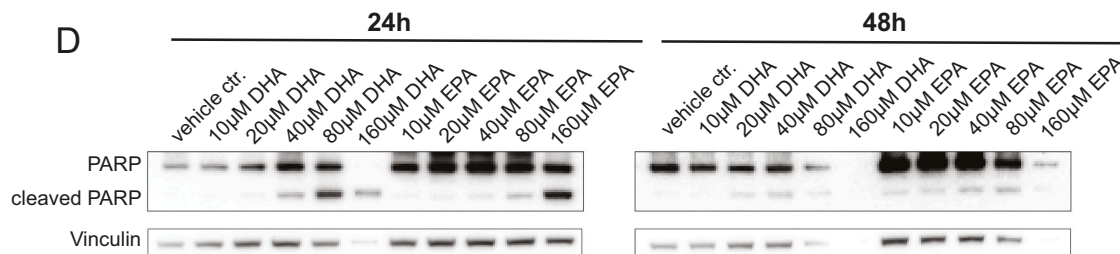
### 3.1. $\omega$ -3-LCPUFA reduces cell viability and induces cell death in MB cell lines and DHA decreases MB cell clonogenicity and reduces PGE<sub>2</sub> levels in MB cell supernatants

The effect of increasing concentration of DHA or EPA on MB cell growth was assessed using the WST-1 cell viability assay in a panel of six human MB cell lines. The used concentrations have previously been established as non-toxic to non-cancerous cells [29]. The data revealed a decrease in cell viability in a concentration-dependent manner after incubation with EPA and DHA for 72 h (Fig. 1A, B). The calculated IC<sub>50</sub> values ranged from 3.83–74.3  $\mu$ M for EPA and 1.93–40.3  $\mu$ M for DHA in the six different cell lines (Fig. 1C). DHA yielded a lower IC<sub>50</sub> comparing



**C Cytotoxic activity as IC<sub>50</sub> µM with SEM**

	EPA	DHA	Comparison of IC <sub>50</sub> DHA vs EPA
<b>DAOY</b>	12.2 ± 1.11	7.85 ± 0.91	P = 0.011
<b>Med8a</b>	8.53 ± 1.01	5.63 ± 1.42	P = 0.15 (NS)
<b>UW228-3</b>	74.3 ± ND#	40.2 ± 4.40	P = 0.99 (NS)
<b>D283</b>	3.83 ± 0.62	1.93 ± 0.14	P = 0.024
<b>D425</b>	28.8 ± 9.22	11.8 ± 3.27	P = 0.12 (NS)
<b>D458</b>	6.04 ± 0.53	3.63 ± 0.37	P = 0.0058



(caption on next page)

all cell lines (paired *t*-test on log IC<sub>50</sub>, *P* = 0.0005). However, when comparing IC<sub>50</sub> values for EPA and DHA in each cell line, the difference was only significant in three cell lines (DAOY, D283 and D458, *t*-test on IC<sub>50</sub> *P* < 0.05, Fig 1C).

To validate the effect on cell death, cleavage of poly (ADP)-ribose polymerase (PARP), a downstream substrate of Caspase-3, was assessed after DHA and EPA treatment using Western blot. Cleaved PARP was detected in DAOY cell lysates following DHA or EPA treatment at 40 µM

**Fig. 1.** EPA and DHA reduce cell viability, clonogenicity and PGE<sub>2</sub> secretion in MB cell lines.

Concentration-effect curves from assessment of cell viability in six MB cell lines after 72 h incubation with increasing concentrations of (A) EPA or (B) DHA (0.625–80.0 μM). Data is presented as mean ± SEM. (C) IC<sub>50</sub> ± SEM from data shown in A-B. In addition, *P* values for comparison of DHA and EPA in each cell line are provided. # SEM for IC<sub>50</sub> could not be determined. Viability was assessed by WST-1. Each concentration was tested in triplicate and the experiment was performed at least three times (A-C). (D) Protein expression of full-length PARP (upper band, 116 kDa) and cleaved PARP (lower band, 89 kDa) in DAOY cells after 24 h treatment with 40–160 μM of EPA or DHA. Vinculin was used as loading control (124 kDa). Protein expression was determined by Western blot analysis. (E) DHA reduced the clonogenicity of DAOY and UW-228-3 cells, presented as % of control. Each concentration was tested in triplicate and mean ± SEM from three independent experiments is displayed. DAOY; ANOVA \*\*\*, Dunnett's MC test CTRL vs DHA; 10 μM \*, 20 μM \*\*, 40 μM \*\*, UW228-3; ANOVA \*\*, Dunnett's MC test CTRL vs DHA; 160 μM \*\*. (F) PGE<sub>2</sub> concentrations in the supernatant from MB cell lines (DAOY, D283) treated with DHA. The cells were pre-incubated with AA for 24 h and thereafter treated for 24 h with DHA (5, 10 or 20 μM). We observed lower PGE<sub>2</sub> concentrations in the supernatant of DHA-treated cells compared to untreated control cells. PGE<sub>2</sub> was measured with ELISA and data is presented as mean ± SD, ANOVA and Dunnett's MC test; DAOY \*\*, CTRL vs DHA; 5 μM \*\*, 10 μM \*\*, 20 μM \*\*, D283 \*\*, CTRL vs DHA; 5 μM \*\*, 10 μM \*\*, 20 μM \*\*. Data from one representative experiment is shown and repeated with similar result. (\**P* < 0.05, \*\**P* < 0.01). NS not significant.

or higher concentrations after 24 h and to a lesser extent after 48 h, although it should be noted that after 48 h only few living cells remained after treatment with 80 and 160 μM DHA and EPA (Fig. 1D, Fig. S1, original blots Fig. S2). Moreover, DHA decreased the colony forming ability of adherent MB cells, DAOY and UW228-3, in a concentration-dependent manner (Fig. 1E, Fig. S3).

To investigate the possible effects on PGE<sub>2</sub> production after ω3-LCPUFA exposure in MB we treated MB cells with DHA after pre-exposure to AA and analyzed PGE<sub>2</sub> levels with ELISA. We observed lower PGE<sub>2</sub> concentrations in the supernatant of DHA-treated MB cells compared to control cells (Fig. 1F).

The effect of DHA and EPA was also assessed in a 3D MB spheroid model where increasing concentrations resulted in significant cell death, visualized by SYTOX™ Green Nucleic Acid Stain and the Incucyte® S3 Live-Cell Analysis instrument (Fig. 2A-C). Cell viability measurements in MB spheroids using CellTiter-Glo® 3D Cell Viability Assay confirmed a decrease in viability following DHA or EPA treatment that was, however, only evident at the highest concentrations (Fig. S4).

### 3.2. DHA impairs tumor growth in a MB xenograft model

To investigate the therapeutic effect of DHA on MB growth *in vivo*,

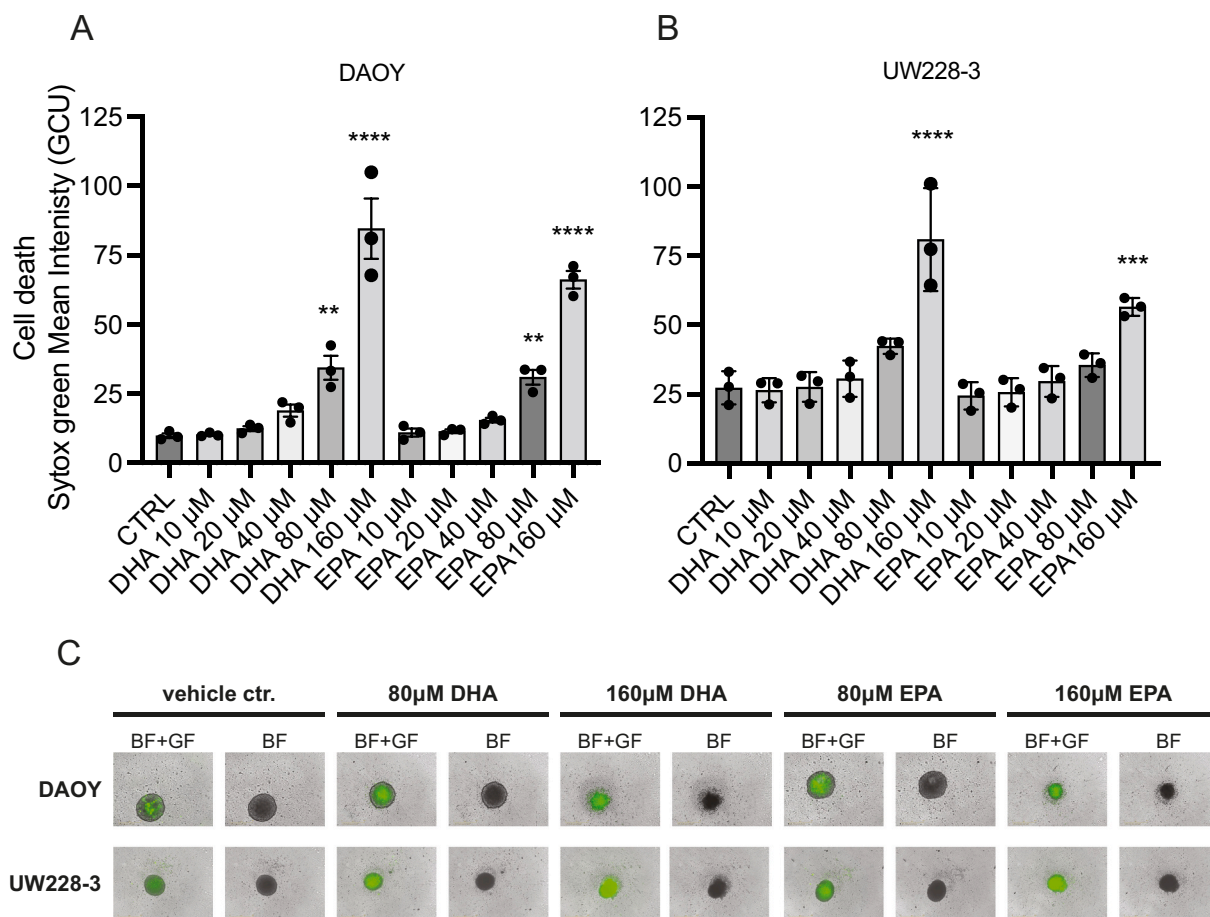


**Fig. 2.** EPA and DHA induce cell death in 3D MB spheroid model.

3D tumor spheroids of (A) DAOY and (B) UW228-3 cells were incubated with increasing concentrations of EPA or DHA (10–160 μM) for 2 cycles of 72 h and cell death was thereafter assessed using SYTOX™ Green. Here presented as average green fluorescence intensity (GCU: Green calibrated Unit), % of control, mean ± SEM from three independent experiments where each concentration was tested in five replicates. ANOVA and Dunnett's MC test; DAOY \*\*\*\* CTRL vs DHA 80 μM \*\* and 160 μM \*\*\*\*, EPA 80 μM \*\* and 160 μM \*\*\*\* respectively, UW228-3 \*\*\*\* CTRL vs DHA 160 μM \*\*\*\*, EPA 160 μM \*\*\*. (C) Images on tumor spheroids from A and B, from bright field (BF) and green fluorescence (GF) channels taken with the Incucyte® S3 using the 10× objective. Green intensity representing dying cells. (\*\**P* < 0.001, \*\*\**P* < 0.001 and \*\*\*\**P* < 0.0001). (For interpretation of the references to color in this figure legend, the reader is referred to the web version of this article.)

nude mice carrying DAOY xenografts were treated with either DHASCO oil (group<sub>DHA</sub>) daily orally (by gastric feeding), FO enriched fruit juice (group<sub>FO</sub>) or no treatment (group<sub>CTRL</sub>). Tumor growth, measured as tumor volume, was significantly decreased in the group<sub>DHA</sub> at day 30 (Fig. 3A). However, no significant change was seen in the tumor volume in the group<sub>FO</sub> compared to the group<sub>CTRL</sub> (Fig. 3A). One tumor in group<sub>DHA</sub> regressed and was not palpable at day 28. Tumor weights at sacrifice displayed no significant differences (Fig. S5). There was no toxicity, assessed as general health and body weight, recorded in any of the three groups during the study (body weight development during the study Fig. S6). However, one mouse was sacrificed in the group<sub>CTRL</sub> at day 22 due to poor health, in accordance with pre-established humane endpoints.

### 3.3. $\omega$ 3-LCPUFA treatment reduces prostanoid concentrations in MB xenografts

To further study the effect from DHA on prostaglandins we analyzed prostanoids in the tumor tissue. We observed significantly lower PGE<sub>2</sub> levels (pmol/mg) in both treatment groups (Fig. 3B) compared to the control group. 6-keto-prostacyclin F<sub>1 $\alpha$</sub>  (6kPGF<sub>1 $\alpha$</sub> ), a stable metabolite of prostacyclin (PGI<sub>2</sub>), was significantly decreased in both treatment groups. Thromboxane B<sub>2</sub> (TxB<sub>2</sub>), a stable metabolite of thromboxane A<sub>2</sub> (TxA<sub>2</sub>), was only significantly decreased in the group<sub>FO</sub>. Of note, one outlier was identified in the DHA oil group and excluded from these analyses (ROUT test, Q = 1%). PGD<sub>2</sub> was not detected in controls or treated tumors.

The ratios between AA, the precursor of PGE<sub>2</sub>, and  $\omega$ 3-docosapentaenoic acid (DPA), the major intermediate of EPA and DHA, and AA/DHA demonstrated a positive Pearson correlation to PGE<sub>2</sub>, AA/DPA ( $P = 0.033$ ,  $r = 0.46$ ) and AA/DHA ( $P = 0.014$ ,  $r = 0.52$ ) (data not shown).

### 3.4. RNA-seq on tumor tissue reveals CRYAB as a new target of $\omega$ 3-LCPUFA

RNA-sequencing on tumor tissue from the xenograft study described above was performed to identify genes and pathways involved in the effect of DHA and FO treatment on MB. Twenty-three genes were downregulated and two genes were upregulated in the group<sub>FO</sub> and 19 genes were downregulated and one gene was upregulated in the group<sub>DHA</sub> (Table S4). Gene set enrichment analysis using hallmarks, kegg, reactome, cgp and, gobp gene sets were performed but yielded no significant results at <25% FDR (data not shown).

The two treatment groups presented 10 downregulated genes in common. The most significantly downregulated gene in both groups was the CRYAB gene (Fig. 3C, Table S4). CRYAB encodes alpha beta crystallin, a heat shock protein previously identified as a prognostic factor in several cancer models [50]. Notably, CRYAB has been shown to act as a pro-survival factor in the brain tumor glioblastoma [51]. This finding on RNA level was confirmed on protein level by immunohistochemistry demonstrating a significant decrease of CRYAB in the  $\omega$ 3-LCPUFA treated tumors compared to the control group (Fig. 3D, E). Another gene that was downregulated in both treatment groups was the apolipoprotein B mRNA editing enzyme catalytic polypeptide 2, APOBEC2. The family of apolipoprotein B mRNA-editing enzyme catalytic subunit (APOBEC) is considered to have important functions in the mutagenesis of genes and thus play a role in several cancers [52–54]. Furthermore, among significantly downregulated genes, ALOX5AP (Arachidonate 5-Lipoxygenase Activating Protein), coding for the enzyme FLAP (5-lipoxygenase-activating protein) was identified in the group<sub>DHA</sub>.

### 3.5. The fatty acid profile in tumor, RBC and brain tissue of $\omega$ 3-treated mice demonstrates differences compared to control animals

Finally, we investigated how the intake of  $\omega$ 3-fatty acids in the treatment groups affected the fatty acid composition of phospholipids in

RBC, tumor, brain and plasma phospholipids (Fig. 4A, B and Table S5).

Analysis of tumor tissue demonstrated a significant increase in EPA and DHA in both treatment groups compared to the controls. In addition, DPA, the major intermediate of EPA and DHA, was increased in both treatment groups compared to the control group, despite small amounts of DPA being present in the supplements. In RBC and plasma, DHA was significantly increased in both treatment groups, whereas EPA increased in the group<sub>FO</sub> only. DPA increased only in the group<sub>FO</sub> in RBC, an increase not seen in plasma. (Table S5). The  $\omega$ 3-index, the sum of EPA and DHA percentage of total fatty acids, and the EDD-index, the sum of EPA, DPA and DHA percentage of total fatty acids, were significantly higher in both treatment groups compared to the control in tumors, brain, RBC and plasma phospholipids (Fig. 4B, Table S5).

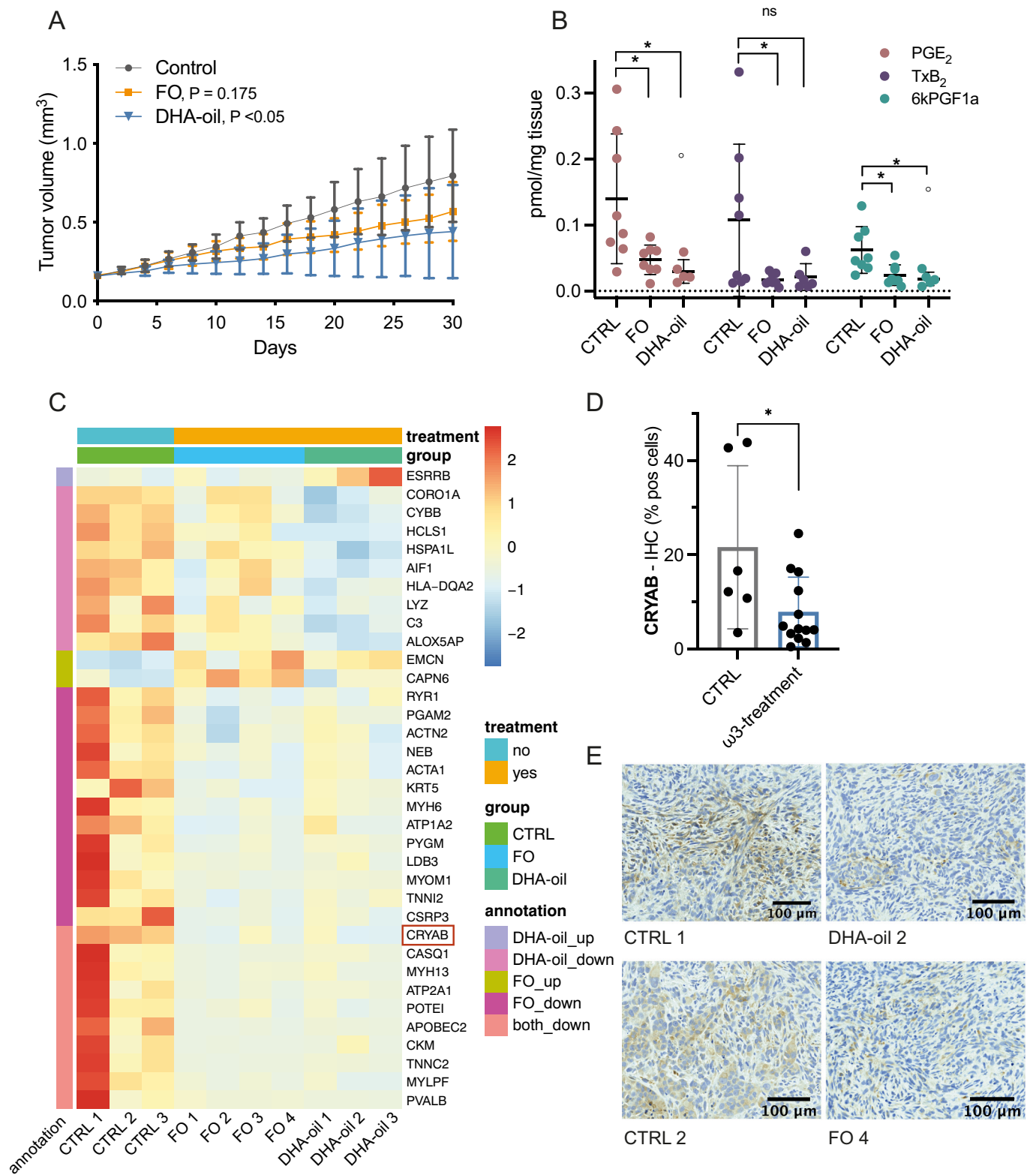
Dihomo- $\gamma$ -linolenic acid (DGLA), the precursor of AA, increased in tumor tissue from both treatment groups compared to the group<sub>CTRL</sub> (Fig. 4A) but was unaffected in RBC (Table S5). Furthermore, the proportion of DGLA in tumor tissue was strongly positively correlated to the proportion of DHA (Pearson correlation:  $P < 0.0001$ ,  $r = 0.92$ ). In addition, AA was significantly lower in RBC from both treatment groups compared to the controls, but not affected in tumor tissues (Table S5). The balance between  $\omega$ 6 and  $\omega$ 3-fatty acids was illustrated by the ratios of AA/EPA, AA/DHA and  $\Sigma\omega$ 6/ $\Sigma\omega$ 3. These ratios were significantly decreased in tumor and RBC from both treatment groups compared to the controls (Fig. 4B, Table S5). Two control tumors were excluded from the AA/EPA analysis in tumor and RBC due to undetectable levels of EPA. Overall, we also observed similar but less pronounced changes in the fatty acids of brain tissue with respect to those seen in tumor (Table S5).

## 4. Discussion

In this study, we present a novel approach to impair growth of MB cells and lower the levels of oncogenic PGE<sub>2</sub> using treatment with the  $\omega$ 3-LCPUFA, DHA and EPA. Our results show that  $\omega$ 3-LCPUFA treatment decreases PGE<sub>2</sub> both *in vitro* and *in vivo* at concentrations that are non-toxic to the mice and convertible to children [42]. Interestingly, the heat shock protein alpha-beta crystallin, CRYAB, was downregulated in the tumor tissue of  $\omega$ 3-LCPUFA treated mice, an effect that has not been described previously.

The potential of using dietary supplementation to lower PGE<sub>2</sub> in tumor tissue, thereby alleviating immune suppression, is of great interest. Beneficial effects have previously been demonstrated for COX inhibitors in combination with both immunotherapy and/or chemotherapy [55,56]. To date, only few clinical trials have explored the potential of lowering PGE<sub>2</sub> by  $\omega$ 3-supplementation in cancer patients. However, one study in patients with varied solid tumors receiving radiation and concomitantly  $\omega$ 3-enriched nutrition for seven days, demonstrated significant reduction in serum PGE<sub>2</sub> levels compared to the controls [57]. Children with MB receive both chemo- and radiotherapy, treatments that have been shown to increase PGE<sub>2</sub> production in glioblastoma, thereby contributing to immunosuppression. Consequently, inhibition of PGE<sub>2</sub> has been shown to mitigate the immune suppression [58]. Of particular interest in the pediatric brain tumor patient cohort is that targeting the PGE<sub>2</sub>/EP2 axis may reverse cognitive decline and attenuate the inflammatory state of the brain [59]. Inhibition of PGE<sub>2</sub>-production or PGE<sub>2</sub>-signaling reduces MB growth [18], and the selective COX-2 inhibitor celecoxib has already been included into a treatment protocol for recurrent or progressive MB (clinicaltrials.gov NCT01356290).

Our study demonstrates that treatment of MB cell lines with DHA and EPA clearly reduced cell viability and induced cell death *in vitro*, both when grown in a 2D setting and as 3D spheroids (Figs. 1, 2). DAOY, the MB cell line used in our *in vitro* and *in vivo* experiments, is well-characterized and has been proposed to belong to the MB<sub>SHH</sub> [36], the group that is associated with an inflammatory profile [10]. Moreover, MB tumors and cell lines have previously been shown to express COX-2,



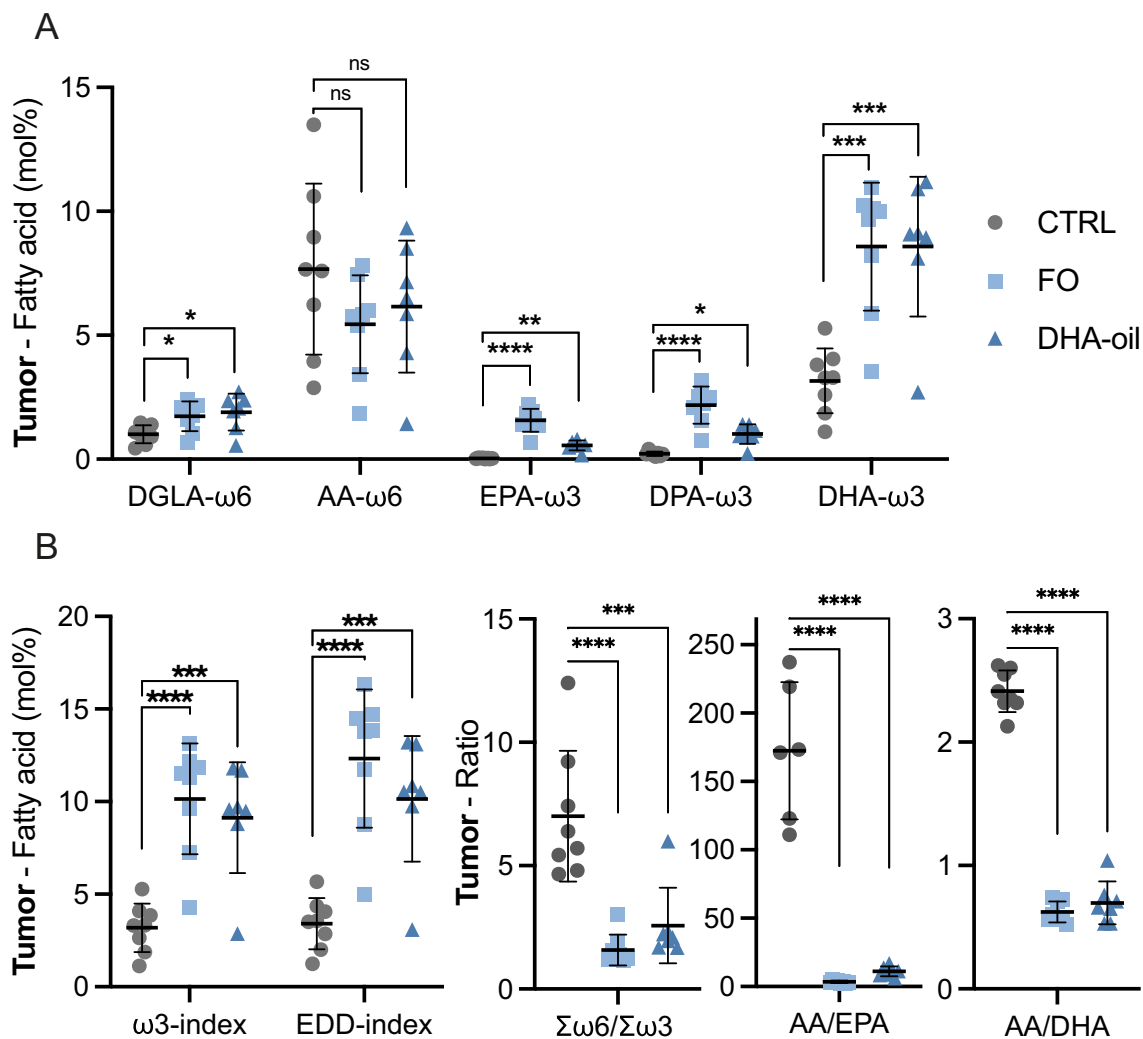
(caption on next page)

mPGES1 and the EP receptors [18]. Furthermore, DHA impaired tumor clone formation at concentrations that are physiologically relevant [60] and non-toxic to normal cells [29]. While the effect was not as pronounced *in vivo*, a significant effect of DHA on tumor growth was observed. Of note, the mice used in this study were immunocompromised, without functional T cells, and an immunocompetent model

would be required to evaluate the full potential of alleviating immunosuppression. The DHA-oil was gavage fed, resulting in daily bolus doses, while the FO resulted in a continuous intake as it replaced the drinking water. The oxidative stress that can be caused by a surplus of ω3-LCPUFA has been suggested to be of importance for their mode of action [30]. While a bolus might cause a significantly high surplus of ω3-

**Fig. 3.**  $\omega$ 3-LCPUFA treatment decreases tumor growth and alters gene expression in MB xenografts.

(A) DHA significantly reduced tumor volume of established MB xenografts (DAOY cells engrafted subcutaneously in NMRI nu/nu mice), comparing CTRL to  $\omega$ 3-treatment (DHA and fish oil (FO) respectively) presented as mean  $\pm$  SD. One-way ANOVA (at day 30) and Dunnett's MC test,  $P = 0.042$ , CTRL vs. DHA:  $P < 0.05$ , CTRL vs FO:  $P = 0.175$ . At established tumor (volume exceeding 150 mm<sup>3</sup>) mice were randomized to one of three treatments groups. Mice were treated for 30 days with DHA oil given daily orally through gastric feeding, FO enriched fruit juice administrated in the drinking bottles ad libitum, or left untreated. (B) Prostanoids (PGE<sub>2</sub>, TxB<sub>2</sub> and 6kPGF1a) in DAOY xenograft tumor tissue from  $\omega$ 3-treated and control mice, measured by LC-MS/MS. A decrease in the concentration of prostanoids was detected in tumors tissue from  $\omega$ 3-treated mice compared to tumors from control mice, ANOVA and Dunnett's MC test: PGE<sub>2</sub> \*\*, group<sub>CTRL</sub> vs. group<sub>FO</sub> \*, group<sub>CTRL</sub> vs group<sub>DHA</sub> \*. TxB<sub>2</sub> \*, group<sub>CTRL</sub> vs F group<sub>FO</sub> \*, group<sub>CTRL</sub> vs group<sub>DHA</sub> ns  $P = 0.0668$ . 6kPGF1 \*\*, group<sub>CTRL</sub> vs group<sub>FO</sub> \*, group<sub>CTRL</sub> vs group<sub>DHA</sub> \*. Outlier marked with a circle. The asterisks represent statistical significance compared to control (\* $P < 0.05$ , \*\* $P < 0.01$  and \*\*\* $P < 0.001$ ). Data presented as mean  $\pm$  SD. (C) Heatmap of up- and down regulated genes assessed by RNA-sequencing, comparing tumors from group<sub>CTRL</sub> vs group<sub>DHA</sub> and group<sub>FO</sub>, presenting upregulated gene expression (red color) and downregulated gene expression (blue color). The expression of the most significantly downregulated gene, *CRYAB* decreased in tumors from group<sub>DHA</sub> (adjusted  $P$  value = 1.59E-10) and group<sub>FO</sub> (adjusted  $P$  value = 2.42E-05), assessed as deviation from average across all samples (highlighted with a red frame). (D, E) *CRYAB* protein expression in tumors from  $\omega$ 3-treated and control mice. The number of positive cells was significantly decreased in tumors from pooled  $\omega$ 3-treated mice compared to group<sub>CTRL</sub>, unpaired  $t$ -test  $P = 0.024$ . *CRYAB* was detected using IHC and the number of *CRYAB*-positive cells in hotspots was determined using QuPath-0.2.3. Mean  $\pm$  SD is presented in (D) and representative images of *CRYAB* protein hotspots in group<sub>CTRL</sub> tumors and  $\omega$ 3-treated tumors in (E). (For interpretation of the references to color in this figure legend, the reader is referred to the web version of this article.)

**Fig. 4.**  $\omega$ 3-treatment changes fatty acid composition in MB xenograft tumors.

$\omega$ 3-treatment resulted in comparable changes in fatty acid composition in tumors from both treatment groups compared to control tumors. (A) The DGLA- $\omega$ 6 and all  $\omega$ 3-LCPUFA (EPA, DPA, DHA) and (B)  $\omega$ 3- and EDD-index increased significantly in tumors from both the DHA and FO treated group when compared with tumors from control mice. Data presented as proportion of total fatty acids (mol%). Ratios illustrating the balance of  $\omega$ 6 and  $\omega$ 3-fatty acids decreased in tumor tissue of  $\omega$ 3-treated mice. One-way ANOVA with Dunnett's MC test comparing tumor tissues from treated mice to tumor tissue from the control, \* $P < 0.05$ , \*\* $P < 0.01$ , \*\*\* $P < 0.001$ , \*\*\*\* $P < 0.0001$ . Data is presented as mean  $\pm$  SD.

LCPUFA, small amounts over time, as will be achieved by the FO, might be manageable for the tumor redox system [40] and also contained a different composition of fatty acids, namely the precursors of LCPUs. Nevertheless, we demonstrate an increase in all three  $\omega$ 3-LCPUFA and a

decrease in PGE<sub>2</sub> in the tumor tissue from  $\omega$ 3-treated mice independent of the treatment strategy. PGE<sub>2</sub> has diverse targets and many downstream effects, both on tumor cells and on other cells in the TME [27,61]. Several effects of PGE<sub>2</sub> inhibition are overlapping with those associated

with  $\omega$ 3-LCPUFA treatment e.g. effects on NF $\kappa$ B and Wnt/ $\beta$ -catenin signaling [30,61,62]. It is probable that the effect on cell viability we observe is multifactorial and complex. We conclude that treatment with  $\omega$ 3-LCPUFA reduced PGE<sub>2</sub> levels in our MB models in agreement with previous report [28]; however, if the observed inhibitory effects on tumor growth are dependent or independent of PGE<sub>2</sub> suppression has yet to be explored.

In line with lower levels of PGE<sub>2</sub>, we observed lower concentrations of the prostacyclin metabolite 6kPGF1 $\alpha$  in both treatment groups, whereas the thromboxane metabolite TxB<sub>2</sub> was lowered in the group<sub>FO</sub> only. This decrease of the three major prostanoids quantified in this study suggests a general inhibition of prostanoid production in the tumor tissue. The mechanisms underlying the observed decrease of prostanoids in the tumor tissue following treatment are likely multifaceted and can be attributed to several  $\omega$ 3-LCPUFA-related mechanisms. For example, it is well-established that DHA competes with AA for incorporation into cell membranes and that  $\omega$ 3-LCPUFA affect the activity of key enzymes in the essential fatty acid transformation and in the AA/COX pathway. In line with this, we observed no impact on the gene expression of enzymes involved in the PGE<sub>2</sub> production pathway. Although DHA is not a substrate for the COX enzymes, it can inhibit COX-mediated AA conversion [63]. It has been demonstrated that the number of double bonds in the  $\omega$ 3-LCPUFA, e.g. DHA, correlates to inhibition of COX-2 activity but not to a reduction in enzyme levels [64]. The incorporation of the PGE<sub>2</sub> substrate AA was significantly lower in both treatment groups in RBC but this effect was not observed in the tumor tissues. The balance of  $\omega$ 6 and  $\omega$ 3 is of importance as a higher AA/EPA ratio, indicating more pro-inflammatory features, has previously been demonstrated in tumor tissue from patients with metastatic disease compared to tumors from patients without metastatic spread [65,66]. Additionally, a lower AA/EPA ratio can dampen the PGE<sub>2</sub> production *in vitro* [67]. In our study, the ratio of AA/DHA and AA/EPA decreased in tumor tissue from both treatment groups (Fig. 3B) and AA/DHA correlated to the PGE<sub>2</sub> levels measured in the tumors.

While both treatments aimed to achieve a comparable intake of total  $\omega$ 3-LCPUFA, the DHA-oil contained DHA only, whereas the FO contained both EPA, DHA and small amount of other  $\omega$ 3-fatty acids like DPA. Interestingly, despite the difference in  $\omega$ 3-LCPUFA composition in the supplements, both EPA and DPA increased significantly in the tumor tissue but not in RBC. Only DHA demonstrated an increase in all tissues to the same extent in both treatment groups, suggesting a level of saturation of DHA in the tissue. Although EPA and DPA were absent in the DHA-oil, their increase in the tissues following treatment could be attributed to retroconversion of DHA to EPA and further conversion to DPA [68]. The interest in DPA, the major intermediate of EPA and DHA, in the context of cancer has increased in recent years as it sensitizes tumor cells to chemotherapy [69] and has been associated with a lower risk of cancer-related mortality [32]. In addition, the proposed role of DPA to act as a reservoir for both EPA and DHA [70] motivates the use of the EDD-index, which includes all three  $\omega$ 3-LCPUFA, distinguishing it from the  $\omega$ 3-index, including only DHA and EPA, when assessing effect of  $\omega$ 3-LCPUFA supplementation [42]. Of note, the increase of EPA and DPA observed in both tumor and brain tissue from the treatment groups was not seen in the RBC or plasma phospholipids of the group<sub>DHA</sub>. However, the group<sub>FO</sub> presented an increase of EPA and DPA in RBC whereas EPA, but not DPA, increased in plasma phospholipids. This emphasizes the importance of assessing the target tissue for the evaluation of effect.

Interestingly, the  $\omega$ 6-fatty acid DGLA increased significantly in tumor tissues from treated mice. DGLA and its metabolites are considered to exert potent anti-inflammatory properties [71] competing with AA and EPA for the COX enzymes and, importantly, DGLA is the precursor of prostaglandin E1 (PGE<sub>1</sub>), for which opposing effects to PGE<sub>2</sub> has been proposed [72]. Recent studies demonstrate that DGLA impairs tumor growth in different cancer models including pancreatic, colon and breast cancer [73–75], and that exogenous addition of DGLA to cancer

cells can result in ferroptosis [76]. Furthermore, PGE<sub>1</sub> has been demonstrated to inhibit MB growth through inhibition of the glioma-associated oncogene, GLI2 activation in the SHH pathway, thereby overcoming drug resistance mechanisms and impeding tumor growth [77].

RNA-sequencing data demonstrated that the expression of relatively few genes were affected by the treatments and a large portion of the downregulated genes were identified in tumors from both treatment groups. CRYAB, a protein with multiple functions in tumorigenesis, emerged as a novel target of  $\omega$ 3-LCPUFA. It was downregulated on both RNA and protein level in the tumor tissue of  $\omega$ 3-LCPUFA-treated mice. CRYAB is reported to have anti-apoptotic effects with cytoprotective abilities as well as pro-angiogenic and pro-metastatic properties [78,79]. Furthermore, CRYAB has been identified as a prognostic factor in several cancer models and a meta-analysis showed that increased CRYAB expression could serve as a biomarker for poor survival in patients with different solid tumors [50,80]. In glioblastoma, CRYAB has been shown to function as a pro-survival factor [50,51] and promote invasion and metastasis [81]. However, contradicting reports indicate that CRYAB also could function as a tumor suppressor in some cancers [82,83]. Despite the potential tumor promoting effects of CRYAB in cancer, the underlying mechanisms are poorly understood. A lung cancer study suggested an interaction with tumor associated macrophages (TAM) [84]. When co-cultured with tumor cells, TAMs promoted invasion by upregulating the CRYAB expression in the tumor cells and activated the ERK signaling pathway [84]. Which role CRYAB has in MB and potential connections to tumor inflammation remains to be studied. Moreover, *APOBEC2*, a nucleic acid editor, was downregulated in both treatment groups and has been implicated in the development of lung and liver cancer and is induced by pro-inflammatory cytokine stimulation and activation of nuclear factor  $\kappa$ B [53,54]. RNA-sequencing of tumor tissue did not reveal a downregulation in genes connected to enzymes in the  $\omega$ 6- or  $\omega$ 3-metabolizing pathway, except for *ALOX5AP*, which was only seen in the DHA-oil group. *ALOX5AP* encodes the FLAP enzyme and is required for AA conversion to leukotrienes by 5-lipoxygenase. *ALOX5AP* has been suggested to be a negative prognostic marker in low-grade glioma [85].

This study has several limitations. Established cell lines cannot fully represent primary MB tumors and lack interaction with the TME. Furthermore, using subcutaneously engrafted xenografts in immunocompromised mice as an *in vivo* model for a brain tumor has disadvantages. The function of the unique immune environment in the CNS is lacking, and a potential effect alleviating immunosuppression cannot be fully evaluated in an immunodeficient strain lacking T-cells. Of note, PGE<sub>2</sub> is known to counteract effector T cells [55,86]. The potential benefit of alleviating immunosuppression and restoring the cancer immunity cycle may be lost thereby potentially mitigating the overall effect of the fatty acids. Follow-up studies in immunocompetent mice, preferable an orthotopically engrafted or transgenic MB model, would be relevant to further investigate the effects of  $\omega$ 3-supplementation on the TME and immune responses in MB.

In conclusion, our studies demonstrate that  $\omega$ 3-LCPUFA exerted cytotoxic effects on MB cells *in vitro* and that DHA-oil reduced tumor growth in a MB xenograft model. Moreover,  $\omega$ 3-LCPUFA decreased PGE<sub>2</sub> both *in vitro* and *in vivo* at concentrations that were non-toxic to the mice. Our data suggests that changes in the balance of AA and  $\omega$ 3-LCPUFA affect the availability of substrates and increase competition of the substrates for PGE<sub>2</sub> production via the COX/mPGES-1 axis. Additionally, tumors from  $\omega$ 3-LCPUFA-treated mice demonstrated a decreased expression of CRYAB, an effect that has not previously been described. Collectively, our findings suggest that  $\omega$ 3-LCPUFA could support MB therapies as they may inhibit immune-suppressing inflammation. Follow-up studies are needed to further elucidate these results and to translate our finding into a clinical setting.

Supplementary data to this article can be found online at <https://doi.org/10.1016/j.lfs.2022.120394>.

## Acknowledgments

We would like to thank to Anna Malmerfelt and Lotta Elfman for their technical assistance. We would also like to acknowledge BEA, the core facility for Bioinformatics and Expression Analysis (supported by the board of research at the Karolinska Institutet and the research committee at the Karolinska University Hospital) for RNA-sequencing. The graphical abstract was created with BioRender.com. This work was supported by The Swedish Childhood Cancer Fund (TJ2016-0058, PR2017-0052, PR2020-0017, TJ2016-0039, PR2015-0098, NCP2016-0021, PR2017-0122); The Swedish Cancer Society (CAN2017/658, 20 0828 PjF, 21 0313 SIA 01H, 19 0566); The Cancer Research Funds of Radiumhemmet/King Gustaf V Jubilee Fund (no 18419, 214163); Mary Béves Forskningsstiftelse; Märta och Gunnar V Philipsons Foundation; The Swedish Foundation for Strategic Research. Thank you to DSM for kindly providing DHASCO oil and Smartfish AS for providing the FO enriched juice.

## References

- [1] E. Bouffet, Management of high-risk medulloblastoma, *Neurochirurgie* 67 (2021) 61–68.
- [2] N.G. Gottardo, A. Gajjar, Current therapy for medulloblastoma, *Curr. Treat. Options Neurol.* 8 (4) (2006) 319–334.
- [3] A.A. King, K. Seidel, C. Di, W.M. Leisenring, S.M. Perkins, K.R. Krull, et al., Long-term neurologic health and psychosocial function of adult survivors of childhood medulloblastoma/PNET: a report from the childhood cancer survivor study, *Neuro-Oncology* 19 (5) (2017) 689–698.
- [4] M. Sabel, G. Fleischhack, S. Tippelt, G. Gustafsson, F. Doz, R. Kortmann, et al., Relapse patterns and outcome after relapse in standard risk medulloblastoma: a report from the HIT-SIOP-PNET4 study, *J. Neuro-Oncol.* 129 (3) (2016) 515–524.
- [5] M. Kool, A. Korshunov, M. Remke, D.T. Jones, M. Schlanstein, P.A. Northcott, et al., Molecular subgroups of medulloblastoma: an international meta-analysis of transcriptome, genetic aberrations, and clinical data of WNT, SHH, group 3, and group 4 medulloblastomas, *Acta Neuropathol.* 123 (4) (2012) 473–484.
- [6] P.A. Northcott, I. Buchhalter, A.S. Morrissy, V. Hovestadt, J. Weischenfeldt, T. Ehrenberger, et al., The whole-genome landscape of medulloblastoma subtypes, *Nature* 547 (7663) (2017) 311–317.
- [7] V. Hovestadt, K.S. Smith, L. Bihannic, M.G. Filbin, M.L. Shaw, A. Baumgartner, et al., Resolving medulloblastoma cellular architecture by single-cell genomics, *Nature* 572 (7767) (2019) 74–79.
- [8] V. Hovestadt, O. Ayrault, F.J. Swartling, G.W. Robinson, S.M. Pfister, P. A. Northcott, Medulloblastomas revisited: biological and clinical insights from thousands of patients, *Nat. Rev. Cancer* 20 (1) (2020) 42–56.
- [9] K.A. Riemondy, S. Venkataraman, N. Willard, A. Nellan, B. Sanford, A. M. Griesinger, et al., Neoplastic and immune single cell transcriptomics define subgroup-specific intra-tumoral heterogeneity of childhood medulloblastoma, *Neuro-Oncology* 24 (2022) 273–286.
- [10] C.D. Pham, C. Flores, C. Yang, E.M. Pinheiro, J.H. Yearley, E.J. Sayour, et al., Differential immune microenvironments and response to immune checkpoint blockade among molecular subtypes of murine medulloblastoma, *Clin. Cancer Res.* 22 (3) (2016) 582–595.
- [11] B. Cen, J.D. Lang, Y. Du, J. Wei, Y. Xiong, N. Bradley, et al., Prostaglandin E2 induces MIR675-5p to promote colorectal tumor metastasis via modulation of p53 expression, *Gastroenterology* 158 (2020) 971–984, e10.
- [12] S. Shalapour, M. Karin, Immunity, inflammation, and cancer: an eternal fight between good and evil, *J. Clin. Invest.* 125 (9) (2015) 3347–3355.
- [13] W.L. Smith, Y. Urade, P.J. Jakobsson, Enzymes of the cyclooxygenase pathways of prostanoid biosynthesis, *Chem. Rev.* 111 (10) (2011) 5821–5865.
- [14] K. Yoshimatsu, N.K. Altorki, D. Golijanin, F. Zhang, P.J. Jakobsson, A. J. Dannenberg, et al., Inducible prostaglandin E synthase is overexpressed in non-small cell lung cancer, *Clin. Cancer Res.* 7 (9) (2001) 2669–2674.
- [15] H.W. Wang, C.T. Hsueh, C.F. Lin, T.Y. Chou, W.H. Hsu, L.S. Wang, et al., Clinical implications of microsomal prostaglandin synthase-1 overexpression in human non-small-cell lung cancer, *Ann. Surg. Oncol.* 13 (9) (2006) 1224–1234.
- [16] K. Larsson, A. Kock, H. Idborg, M. Arsenian Henriksson, T. Martinsson, J. I. Johnsen, et al., COX/mPGES-1/PGE2 pathway depicts an inflammatory-dependent high-risk neuroblastoma subset, *Proc. Natl. Acad. Sci. U. S. A.* 112 (26) (2015) 8070–8075.
- [17] S. Mehrotra, A. Morimiya, B. Agarwal, R. Konger, S. Badve, Microsomal prostaglandin E2 synthase-1 in breast cancer: a potential target for therapy, *J. Pathol.* 208 (3) (2006) 356–363.
- [18] N. Baryawno, B. Sveinbjornsson, S. Eksborg, A. Orrego, L. Segerstrom, C.O. Oqvist, et al., Tumor-growth-promoting cyclooxygenase-2 prostaglandin E2 pathway provides medulloblastoma therapeutic targets, *Neuro-Oncology* 10 (5) (2008) 661–674.
- [19] S. Tomic, B. Joksimovic, M. Bekic, M. Vasiljevic, M. Milanovic, M. Colic, et al., Prostaglandin-E2 potentiates the suppressive functions of human mononuclear myeloid-derived suppressor cells and increases their capacity to expand IL-10-producing regulatory T cell subsets, *Front. Immunol.* 10 (2019) 475.
- [20] H. Harizi, M. Juzan, V. Pitard, J.F. Moreau, N. Gualde, Cyclooxygenase-2-issued prostaglandin e(2) enhances the production of endogenous IL-10, which down-regulates dendritic cell functions, *J. Immunol.* 168 (5) (2002) 2255–2263.
- [21] Y.M. Mao, D. Sarhan, A. Steven, B. Seliger, R. Kiessling, A. Lundqvist, Inhibition of tumor-derived prostaglandin-E2 blocks the induction of myeloid-derived suppressor cells and recovers natural killer cell activity, *Clin. Cancer Res.* 20 (15) (2014) 4096–4106.
- [22] Y. Zheng, V. Comaills, R. Burr, G. Boulay, D.T. Miyamoto, B.S. Wittner, et al., COX-2 mediates tumor-stromal prolactin signaling to initiate tumorigenesis, *Proc. Natl. Acad. Sci. U. S. A.* 116 (12) (2019) 5223–5232.
- [23] J. Qiu, Z. Shi, J. Jiang, Cyclooxygenase-2 in glioblastoma multiforme, *Drug Discov. Today* 22 (1) (2017) 148–156.
- [24] E. Sandén, S. Eberstål, E. Visse, P. Siesjö, A. Darabi, A standardized and reproducible protocol for serum-free monolayer culturing of primary paediatric brain tumours to be utilized for therapeutic assays, *Sci. Rep.* 5 (2015) 12218.
- [25] K.H. Chen, C.C. Hsu, W.S. Song, C.S. Huang, C.C. Tsai, C.D. Kuo, et al., Celecoxib enhances radiosensitivity in medulloblastoma-derived CD133-positive cells, *Childs Nerv. Syst.* 26 (11) (2010) 1605–1612.
- [26] M.J. Jiang, D.N. Gu, J.J. Dai, Q. Huang, L. Tian, Dark side of cytotoxic therapy: chemoradiation-induced cell death and tumor repopulation, *Trends Cancer* 6 (5) (2020) 419–431.
- [27] A.V. Kurtova, J. Xiao, Q. Mo, S. Pazhanisamy, R. Krasnow, S.P. Lerner, et al., Blocking PGE2-induced tumour repopulation abrogates bladder cancer chemoresistance, *Nature* 517 (7533) (2015) 209–213.
- [28] H. Gleissman, R. Yang, K. Martinod, M. Lindskog, C.N. Serhan, J.I. Johnsen, et al., Docosahexaenoic acid metabolome in neural tumors: identification of cytotoxic intermediates, *FASEB J.* 24 (3) (2010) 906–915.
- [29] M. Lindskog, H. Gleissman, F. Ponthan, J. Castro, P. Kogner, J.I. Johnsen, Neuroblastoma cell death in response to docosahexaenoic acid: sensitization to chemotherapy and arsenic-induced oxidative stress, *Int. J. Cancer* 118 (10) (2006) 2584–2593.
- [30] D. D'Eliseo, F. Velotti, Omega-3 fatty acids and cancer cell cytotoxicity: implications for multi-targeted cancer therapy, *J. Clin. Med.* 5 (2) (2016).
- [31] E. Dierge, E. Debock, C. Guilbaud, C. Corbet, E. Mignolet, L. Mignard, et al., Peroxidation of n-3 and n-6 polyunsaturated fatty acids in the acidic tumor environment leads to ferroptosis-mediated anticancer effects, *Cell Metab.* 33 (8) (2021) 1701–1715, e5.
- [32] W.S. Harris, N.L. Tintle, F. Imamura, F. Qian, A.V.A. Korat, M. Marklund, et al., Blood n-3 fatty acid levels and total and cause-specific mortality from 17 prospective studies, *Nat. Commun.* 12 (1) (2021) 2329.
- [33] L. Wei, Z. Wu, Y.Q. Chen, Multi-targeted therapy of cancer by omega-3 fatty acids-an update, *Cancer Lett.* 526 (2021) 193–204.
- [34] M. Montecillo-Aguado, B. Tirado-Rodriguez, Z. Tong, O.M. Vega, M. Morales-Martínez, S. Abkenari, et al., Importance of the role of ω-3 and ω-6 polyunsaturated fatty acids in the progression of brain cancer, *Brain Sci.* 10 (6) (2020).
- [35] F. Wang, K. Bhat, M. Doucette, S. Zhou, Y. Gu, B. Law, et al., Docosahexaenoic acid (DHA) sensitizes brain tumor cells to etoposide-induced apoptosis, *Curr. Mol. Med.* 11 (6) (2011) 503–511.
- [36] D.P. Ivanov, B. Coyle, D.A. Walker, A.M. Grabowska, In vitro models of medulloblastoma: choosing the right tool for the job, *J. Biotechnol.* 236 (2016) 10–25.
- [37] S.J. Roper, F. Linke, P.J. Scotting, B. Coyle, 3D spheroid models of paediatric SHH medulloblastoma mimic tumour biology, drug response and metastatic dissemination, *Sci. Rep.* 11 (1) (2021) 4259.
- [38] N.A. Franken, H.M. Rodermond, J. Stap, J. Haveman, C. van Bree, Clonogenic assay of cells in vitro, *Nat. Protoc.* 1 (5) (2006) 2315–2319.
- [39] E. Wassberg, S. Pählman, J.E. Westlin, R. Christofferson, The angiogenesis inhibitor TNP-470 reduces the growth rate of human neuroblastoma in nude rats, *Pediatr. Res.* 41 (3) (1997) 327–333.
- [40] H. Gleissman, L. Segerstrom, M. Hamberg, F. Ponthan, M. Lindskog, J.I. Johnsen, et al., Omega-3 fatty acid supplementation delays the progression of neuroblastoma in vivo, *Int. J. Cancer* 128 (7) (2011) 1703–1711.
- [41] A.B. Nair, S. Jacob, A simple practice guide for dose conversion between animals and human, *J. Basic Clin. Pharm.* 7 (2) (2016) 27–31.
- [42] L. Ljungblad, H. Gleissman, G. Hedberg, M. Wickström, N. Eissler, J. Pickova, et al., Body surface area-based omega-3 fatty acids supplementation strongly correlates to blood concentrations in children, *Prostaglandins Leukot. Essent. Fat. Acids* 169 (2021), 102285.
- [43] A. Hara, N.S. Radin, Lipid extraction of tissues with a low-toxicity solvent, *Anal. Biochem.* 90 (1) (1978) 420–426.
- [44] K.P. Grawé, J. Pickova, P.C. Dutta, A. Oskarsson, Fatty acid alterations in liver and milk of cadmium exposed rats and in brain of their suckling offspring, *Toxicol. Lett.* 148 (1–2) (2004) 73–82.
- [45] H. Idborg, P. Olsson, P. Leclerc, J. Raouf, P.J. Jakobsson, M. Korotkova, Effects of mPGES-1 deletion on eicosanoid and fatty acid profiles in mice, *Prostaglandins Other Lipid Mediat.* 107 (2013) 18–25.
- [46] A. Dobin, C.A. Davis, F. Schlesinger, J. Drenkow, C. Zaleski, S. Jha, et al., STAR: ultrafast universal RNA-seq aligner, *Bioinformatics* 29 (1) (2013) 15–21.
- [47] S. Anders, P.T. Pyl, W. Huber, HTSeq—a python framework to work with high-throughput sequencing data, *Bioinformatics* 31 (2) (2015) 166–169.
- [48] M.I. Love, W. Huber, S. Anders, Moderated estimation of fold change and dispersion for RNA-seq data with DESeq2, *Genome Biol.* 15 (12) (2014) 550.
- [49] P. Bankhead, M.B. Loughrey, J.A. Fernández, Y. Dombrowski, D.G. McArt, P. D. Dunne, et al., QuPath: open source software for digital pathology image analysis, *Sci. Rep.* 7 (1) (2017) 16878.

- [50] X. Tao, L. Cheng, Y. Li, H. Ci, J. Xu, S. Wu, et al., Expression of CRYAB with the angiogenesis and poor prognosis for human gastric cancer, *Medicine (Baltimore)* 98 (45) (2019), e17799.
- [51] E. Hirata, K. Ishibashi, S. Kohsaka, K. Shinjo, S. Kojima, Y. Kondo, The brain microenvironment induces DNMT1 suppression and indolence of metastatic cancer cells, *iScience* 23 (9) (2020), 101480.
- [52] N. Roper, S. Gao, T.K. Maity, A.R. Banday, X. Zhang, A. Venugopalan, et al., APOBEC mutagenesis and copy-number alterations are drivers of proteogenomic tumor evolution and heterogeneity in metastatic thoracic tumors, *Cell Rep.* 26 (10) (2019) 2651–2666, e6.
- [53] S. Okuyama, H. Marusawa, T. Matsumoto, Y. Ueda, Y. Matsumoto, Y. Endo, et al., Excessive activity of apolipoprotein B mRNA editing enzyme catalytic polypeptide 2 (APOBEC2) contributes to liver and lung tumorigenesis, *Int. J. Cancer* 130 (6) (2012) 1294–1301.
- [54] T. Matsumoto, H. Marusawa, Y. Endo, Y. Ueda, Y. Matsumoto, T. Chiba, Expression of APOBEC2 is transcriptionally regulated by NF-kappaB in human hepatocytes, *FEBS Lett.* 580 (3) (2006) 731–735.
- [55] V.S. Pelly, A. Moeini, L.M. Roelofsen, E. Bonavita, C.R. Bell, C. Hutton, et al., Anti-inflammatory drugs remodel the tumor immune environment to enhance immune checkpoint blockade efficacy, *Cancer Discov.* 11 (2021) 2602–2619.
- [56] S. Li, M. Jiang, L. Wang, S. Yu, Combined chemotherapy with cyclooxygenase-2 (COX-2) inhibitors in treating human cancers: recent advancement, *Biomed. Pharmacother.* 129 (2020), 110389.
- [57] J. Faber, M. Berkhout, U. Fiedler, M. Avlar, B.J. Witteman, A.P. Vos, et al., Rapid EPA and DHA incorporation and reduced PGE2 levels after one week intervention with a medical food in cancer patients receiving radiotherapy, a randomized trial, *Clin. Nutr.* 32 (3) (2013) 338–345.
- [58] A. Authier, K.J. Farrand, K.W. Broadley, L.R. Ancelet, M.K. Hunn, S. Stone, et al., Enhanced immunosuppression by therapy-exposed glioblastoma multiforme tumor cells, *Int. J. Cancer* 136 (11) (2015) 2566–2578.
- [59] P.S. Minhas, A. Latif-Hernandez, M.R. McReynolds, A.S. Durairaj, Q. Wang, A. Rubin, et al., Restoring metabolism of myeloid cells reverses cognitive decline in ageing, *Nature* 590 (7844) (2021) 122–128.
- [60] A. Rusca, A.F. Di Stefano, M.V. Doig, C. Scarsi, E. Perucca, Relative bioavailability and pharmacokinetics of two oral formulations of docosahexaenoic acid/ eicosapentaenoic acid after multiple-dose administration in healthy volunteers, *Eur. J. Clin. Pharmacol.* 65 (5) (2009) 503–510.
- [61] D. Wang, C.S. Cabalag, N.J. Clemons, R.N. DuBois, Cyclooxygenases and prostaglandins in tumor immunology and microenvironment of gastrointestinal cancer, *Gastroenterology* 161 (6) (2021) 1813–1829.
- [62] M. Xue, Q. Wang, J. Zhao, L. Dong, Y. Ge, L. Hou, et al., Docosahexaenoic acid inhibited the Wnt/ $\beta$ -catenin pathway and suppressed breast cancer cells in vitro and in vivo, *J. Nutr. Biochem.* 25 (2) (2014) 104–110.
- [63] E.J. Corey, C. Shih, J.R. Cashman, Docosahexaenoic acid is a strong inhibitor of prostaglandin but not leukotriene biosynthesis, *Proc. Natl. Acad. Sci. U. S. A.* 80 (12) (1983) 3581–3584.
- [64] P.C. Norris, E.A. Dennis, Omega-3 fatty acids cause dramatic changes in TLR4 and purinergic eicosanoid signaling, *Proc. Natl. Acad. Sci. U. S. A.* 109 (22) (2012) 8517–8522.
- [65] V. Tutino, V. De Nunzio, M.G. Caruso, N. Veronese, D. Lorusso, M. Di Masi, et al., Elevated AA/EPA ratio represents an inflammatory biomarker in tumor tissue of metastatic colorectal cancer patients, *Int. J. Mol. Sci.* 20 (8) (2019).
- [66] M. Notarnicola, D. Lorusso, V. Tutino, V. De Nunzio, G. De Leonardi, G. Marangelli, et al., Differential tissue fatty acids profiling between colorectal cancer patients with and without synchronous metastasis, *Int. J. Mol. Sci.* 19 (4) (2018).
- [67] M. Wada, C.J. DeLong, Y.H. Hong, C.J. Rieke, I. Song, R.S. Sidhu, et al., Enzymes and receptors of prostaglandin pathways with arachidonic acid-derived versus eicosapentaenoic acid-derived substrates and products, *J. Biol. Chem.* 282 (31) (2007) 22254–22266.
- [68] H.W. Sprecher, S.P. Baykousheva, D.L. Luthria, B.S. Mohammed, Differences in the regulation of biosynthesis of 20- versus 22-carbon polyunsaturated fatty acids, *Prostaglandins Leukot. Essent. Fat. Acids* 52 (2–3) (1995) 99–101.
- [69] F.J. Dijk, M. van Dijk, B. Dorresteijn, K. van Norren, DPA shows comparable chemotherapy sensitizing effects as EPA upon cellular incorporation in tumor cells, *Oncotarget* 10 (57) (2019) 5983–5992.
- [70] X.F. Guo, W.F. Tong, Y. Ruan, A.J. Sinclair, D. Li, Different metabolism of EPA, DPA and DHA in humans: a double-blind cross-over study, *Prostaglandins Leukot. Essent. Fat. Acids* 158 (2020), 102033.
- [71] E. Novichkova, K. Chumin, N. Eretz-Kdosha, S. Boussiba, J. Gopas, G. Cohen, et al., DGLA from the microalga *labyrinthula incisa* P127 modulates inflammatory response, inhibits iNOS expression and alleviates NO secretion in RAW264.7 murine macrophages, *Nutrients* 12 (9) (2020).
- [72] X. Wang, H. Lin, Y. Gu, Multiple roles of dihomogamma-linolenic acid against proliferation diseases, *Lipids Health Dis.* 11 (2012) 25.
- [73] X. Yang, Y. Xu, D. Gao, L. Yang, S.Y. Qian, Dihomo-gamma-linolenic acid inhibits growth of xenograft tumors in mice bearing human pancreatic cancer cells (BxPC-3) transfected with delta-5-desaturase shRNA, *Redox Biol.* 20 (2019) 236–246.
- [74] Y. Xu, X. Yang, T. Wang, L. Yang, Y.Y. He, K. Miskimins, et al., Knockdown delta-5-desaturase in breast cancer cells that overexpress COX-2 results in inhibition of growth, migration and invasion via a dihomogamma-linolenic acid peroxidation dependent mechanism, *BMC Cancer* 18 (1) (2018) 330.
- [75] Y. Xu, X. Yang, P. Zhao, Z. Yang, C. Yan, B. Guo, et al., Knockdown of delta-5-desaturase promotes the anti-cancer activity of dihomogamma-linolenic acid and enhances the efficacy of chemotherapy in colon cancer cells expressing COX-2, *Free Radic. Biol. Med.* 96 (2016) 67–77.
- [76] M.A. Perez, L. Magtanong, S.J. Dixon, J.L. Watts, Dietary lipids induce ferroptosis in caenorhabditis elegans and human cancer cells, *Dev. Cell* 54 (4) (2020) 447–454, e4.
- [77] F. Wu, C. Zhang, C. Zhao, H. Wu, Z. Teng, T. Jiang, et al., Prostaglandin E1 inhibits GLI2 amplification-associated activation of the hedgehog pathway and drug refractory tumor growth, *Cancer Res.* 80 (13) (2020) 2818–2832.
- [78] J. Zhang, J. Liu, J. Wu, W. Li, Z. Chen, L. Yang, Progression of the role of CRYAB in signaling pathways and cancers, *Oncotargets Ther.* 12 (2019) 4129–4139.
- [79] D. Caporossi, A. Parisi, C. Fantini, E. Grazioli, C. Cerulli, I. Dimauro, AlphaB-crystallin and breast cancer: role and possible therapeutic strategies, *Cell Stress Chaperones* 26 (1) (2021) 19–28.
- [80] M. Yang, Y. Li, F. Tian, Association between alpha B-crystallin expression and prognosis in patients with solid tumors: a protocol for systematic review and meta-analysis, *Medicine (Baltimore)* 100 (7) (2021), e24831.
- [81] Y. Song, D. Jin, N. Ou, Z. Luo, G. Chen, J. Chen, et al., Gene expression profiles identified novel urine biomarkers for diagnosis and prognosis of high-grade bladder urothelial carcinoma, *Front. Oncol.* 10 (2020) 394.
- [82] H. Ruan, Y. Li, X. Wang, B. Sun, W. Fang, S. Jiang, et al., CRYAB inhibits migration and invasion of bladder cancer cells through the PI3K/AKT and ERK pathways, *Jpn. J. Clin. Oncol.* 50 (3) (2020) 254–260.
- [83] Z. Huang, Y. Cheng, P.M. Chiu, F.M. Cheung, J.M. Nicholls, D.L. Kwong, et al., Tumor suppressor alpha B-crystallin (CRYAB) associates with the cadherin/catenin adherens junction and impairs NPC progression-associated properties, *Oncogene* 31 (32) (2012) 3709–3720.
- [84] Z. Guo, J. Song, J. Hao, H. Zhao, X. Du, E. Li, et al., M2 macrophages promote NSCLC metastasis by upregulating CRYAB, *Cell Death Dis.* 10 (6) (2019) 377.
- [85] M. Zhang, X. Wang, X. Chen, F. Guo, J. Hong, Prognostic value of a stemness index-associated signature in primary lower-grade glioma, *Front. Genet.* 11 (2020) 441.
- [86] Y. Take, S. Koizumi, A. Nagahisa, Prostaglandin E receptor 4 antagonist in cancer immunotherapy: mechanisms of action, *Front. Immunol.* 11 (2020) 324.